

This agrees favorably with the value of 1.6 ± 0.3 which was observed experimentally.

It thus appears that the cross sections for these reactions can be understood in terms of the Laing and Moorhouse approach with the added assumption that the number of initial and final states involved is more important than their detailed nature. So far all of the reactions studied have involved nuclei that are closely related in that they have quite similar mass numbers. It would be of interest to see if this behavior is found for similar reactions involving other nuclei in different regions of the periodic table.

ACKNOWLEDGMENTS

We would like to acknowledge the contribution made by the operating and engineering staff of the 300-MeV betatron facility in making the irradiations possible. The cross sections reported here were calculated from the yield-curve data with the aid of an IBM-7094 computer which was operated by the University of Illinois Digital Computer Laboratory and was supported by a grant from the National Science Foundation. One of us (WBW) held a National Science Foundation predoctoral fellowship during part of the time that this project was worked on.

Study of the $Ca^{40}(d,p)Ca^{41}$ Ground State Reaction at $E_d = 14.3$ MeV*

SVEN A. HJORTH† AND J. X. SALADIN

University of Pittsburgh, Pittsburgh, Pennsylvania

AND

G. R. SATCHLER

Oak Ridge National Laboratory, Oak Ridge, Tennessee

(Received 28 January 1965)

The proton polarization from the $Ca^{40}(d,p)Ca^{41}$ ground-state (g.s.) reaction has been measured in the angular range from 15° to 90° at a mean deuteron energy of 14.3 MeV. The $Ca^{40}(d,d)Ca^{40}$ and the $Ca^{40}(d,p)Ca^{41}$ g.s. differential cross sections were determined at the same bombarding energy and within the same angular range. A preliminary analysis of the data in terms of the distorted-wave Born approximation theory is presented. Most calculations were performed in the zero-range approximation with local optical potentials, but including the effects of nonlocality in the approximation of Perey. The inclusion of finite range improved the fit to the (d,p) cross sections but had little effect on the polarization. Although a good fit to the polarization data has not been obtained, it is clear that a spin-orbit term is needed in the deuteron optical potential, and furthermore, the indications are that the imaginary part of the spin-orbit potential has to be positive or zero.

I. INTRODUCTION

ONE-nucleon transfer reactions have, in recent years, become a very powerful tool in nuclear spectroscopy. These reactions are usually analyzed in terms of the distorted-wave Born approximation (DWBA),¹ which accounts very well for the shape of the differential cross section, particularly at forward angles. This permits in general an unambiguous l -value assignment to the observed level. The absolute cross section, as predicted by the theory however, is rather sensitive to the parameters entering the calculations, and it is well

known that the absolute values of the spectroscopic factors extracted from a DWBA analysis can be in error by as much as 50%. There are also some doubts about the treatment of the nuclear interior; sometimes the agreement with experimental data is improved if a somewhat arbitrary lower cutoff (radius) is employed in the evaluation of the radial integral of the transition amplitude. In light of this situation a very extensive experimental and theoretical study of the $Ca^{40}(d,p)Ca^{41}$ and the $Ca^{40}(d,d)Ca^{40}$ reactions has recently been performed in the energy range between 7 and 12 MeV.^{2,3}

Ca^{40} is a suitable target nucleus to be used as a "calibration point" of the DWBA theory, since the structures of Ca^{40} and Ca^{41} are quite well understood in terms of the shell model and the spectroscopic factors

* Work supported by the National Science Foundation under Grant No. G-11309 and by the U. S. Atomic Energy Commission under contract with the Union Carbide Corporation.

† On leave of absence from the Nobel Institute of Physics, Stockholm, Sweden.

¹ For the basic theory see, for instance, W. Tobocman, *Theory of Direct Nuclear Reactions*, (Oxford University Press, New York, 1961); N. Austern, *Fast Neutron Physics II*, edited by J. B. Marion and J. L. Fowler, (Interscience Publishers, Inc., New York, 1963). For a reference list to applications of the theory, see Ref. 3.

² R. H. Bassel, R. M. Drisko, G. R. Satchler, L. L. Lee, J. P. Schiffer, and B. Zeidman, *Phys. Rev.* **136**, B960 (1964).

³ L. L. Lee, J. P. Schiffer, B. Zeidman, G. R. Satchler, R. M. Drisko, and R. H. Bassel, *Phys. Rev.* **136**, B971 (1964).

S for (d,p) transitions to the $1f_{7/2}$, $2p_{3/2}$, and the $2p_{1/2}$ states in Ca^{41} are expected to be close to unity. It is thus possible to check in this case the reliability with which spectroscopic factors can be extracted from a DWBA calculation.

In the previous investigations,^{2,3} it was found that the calculated (d,p) cross sections depended, among other things, on the spin-orbit parts of the optical potentials. Whereas the spin-orbit term for the proton potential is fairly well determined from the analysis of elastic scattering and polarization data, very little is known about the spin-dependent terms of the deuteron potential. Spin-orbit interactions, however, are known to have a strong influence on the polarization of the outgoing particles. One may thus hope that a measurement of the polarization in the $\text{Ca}^{40}(d,p)\text{Ca}^{41}$ ground-state (g.s.) reaction would help to remove some of the ambiguities in the parameters used in the DWBA calculations.

The proton polarization from the $\text{Ca}^{40}(d,p)\text{Ca}^{41}$ g.s. reaction in the 10-20 MeV range has previously been measured by different groups at 10 MeV,⁴ 10.9 MeV,⁵ 11.4 MeV,⁶ 13.8 MeV,⁷ and 21.0 MeV,⁸ but in view of the importance of this reaction, it was felt that a measurement at 14.3 MeV was well motivated. In order to establish continuity with earlier measurements and make a complete analysis possible, the deuteron-elastic and the ground-state (d,p) cross sections were also determined.

II. EXPERIMENTAL PROCEDURE AND RESULTS

A. The Polarization-Measurements

The experimental arrangement was almost identical to that used previously by Reber *et al.*⁹ and will be described only briefly.

An 18.5 ± 0.8 mg/cm² thick calcium target was rolled from natural calcium (96.97% Ca^{40}) and bombarded with the 14.8-MeV deuteron beam from the University of Pittsburgh cyclotron. Depending on target angle, the energy loss of the deuterons in the target was 0.8 to 1.3 MeV. Protons corresponding to the ground state of Ca^{41} were focused into the polarimeter by means of a 60° homogeneous-field spectrometer. A 130 mg/cm² thick carbon target served as polarization analyzer. The left-right asymmetry in the elastic scattering was determined by means of two counter telescopes located

⁴ R. W. Bercaw and F. B. Shull, Phys. Rev. **133**, B632 (1964).

⁵ S. Kato, N. Takahashi, M. Tahida, T. Yamazaki, and S. Yasukawa, Osaka University Report No. OU-LNS 64-2 1964 (unpublished).

⁶ M. Takeda, S. Kato, C. Hu, and N. Takahashi, in *Proceedings of the International Conference on Nuclear Structure, Kingston, Ontario, 1960* (University of Toronto Press, Toronto, 1960).

⁷ M. V. Pasechnik, L. S. Saltykov, and D. I. Tambovtsev, Zh. Eksperim. i Teor. Fiz. **43**, 1575 (1963) [English transl.: Soviet Phys.—JETP **16**, 1111 (1963)].

⁸ E. Boschitz, in *Proceedings of the Conference on Direct Interactions and Nuclear Reaction Mechanisms, Padua, 1962* (Gordon and Breach Science Publishers, Inc., New York, 1963).

⁹ L. H. Reber and J. X. Saladin, Phys. Rev. **133**, B1155 (1964).

at $\pm 47.5^\circ$ relative to the incident beam. Originally, each of these telescopes consisted of a proportional counter and a CsI scintillation detector. During the course of the present experiment, the proportional counters were substituted by 300 mm², 200 μ -thick completely depleted transmission-mount solid-state detectors. This lowered the background and made the system on the whole more reliable. The pulses from the scintillation counters were gated by the solid-state detector pulses and analyzed in a 4096 channel Nuclear Data pulse-height analyzer. A typical proton spectrum from the right and left counter is shown in Fig. 1. Clearly, there was no problem in separating the proton groups corresponding to elastic and inelastic scattering from the carbon target.

Each polarization measurement consisted of a series of runs, after each of which the polarimeter was rotated 180° about its axis of symmetry. In this way the instrumental asymmetry could be kept below 1% (see Ref. 10 for a detailed discussion). The analyzing power $\langle p_2 \rangle$ of the polarimeter has been calculated previously¹⁰ for proton energies up to 19.5 MeV. By means of recent data at 19.9 MeV,¹¹ these calculations were extrapolated up to 20 MeV. The uncertainty $\delta\langle p_2 \rangle / \langle p_2 \rangle$ in the analyzing power is believed to be smaller than 10%. An error in $\langle p_2 \rangle$ will change the absolute value of the polarization but does not influence the shape of the polarization pattern. The results of the polarization measurements are summarized in Table I; only the statistical errors are quoted. A comparison between the present data and measurements obtained at other energies between 10 and 21 MeV is shown in Fig. 2. The polarization patterns at different energies appear qualitatively similar.

TABLE I. The polarization in $\text{Ca}^{40}(d,p)\text{Ca}^{41}$ g.s. at 14.3 MeV. Only the statistical errors are quoted.

$\theta_{c.m.}$	Asymmetry	E_p^a	$\langle p_2 \rangle$	P
15.4	0.936 ± 0.042	19.8	-0.400	0.083 ± 0.054
20.6	1.070 ± 0.050	19.9	-0.390	-0.087 ± 0.062
25.7 ^b	1.043 ± 0.050	18.9	-0.500	-0.042 ± 0.050
30.9	1.122 ± 0.056	19.8	-0.400	-0.144 ± 0.066
36.0 ^b	1.035 ± 0.050	18.9	-0.500	-0.034 ± 0.050
41.1	1.019 ± 0.045	19.7	-0.415	-0.023 ± 0.054
46.2 ^b	0.950 ± 0.067	18.9	-0.500	$+0.052 \pm 0.068$
51.3	1.060 ± 0.065	19.6	-0.430	-0.068 ± 0.073
56.4	1.514 ± 0.150	18.3	-0.536	-0.381 ± 0.090
61.5	1.368 ± 0.068	19.4	-0.450	-0.345 ± 0.056
66.6	1.113 ± 0.070	18.1	-0.545	-0.098 ± 0.058
71.6	1.022 ± 0.065	19.1	-0.480	-0.023 ± 0.067
81.7	0.987 ± 0.054	19.1	-0.480	$+0.013 \pm 0.054$
91.7	1.341 ± 0.130	19.0	-0.490	-0.297 ± 0.100

^a In some measurements the protons were degraded in energy by means of polyethylene absorbers before they entered the polarimeter.

^b Obtained at 14.7 MeV since in these runs the energy of the cyclotron was 0.4 MeV higher.

¹⁰ L. H. Reber, Ph.D. thesis, University of Pittsburgh, 1963 (unpublished).

¹¹ R. M. Craig, J. C. Dore, G. W. Greenlees, J. S. Lilley, and P. C. Rowe, Phys. Letters **3**, 301 (1963).

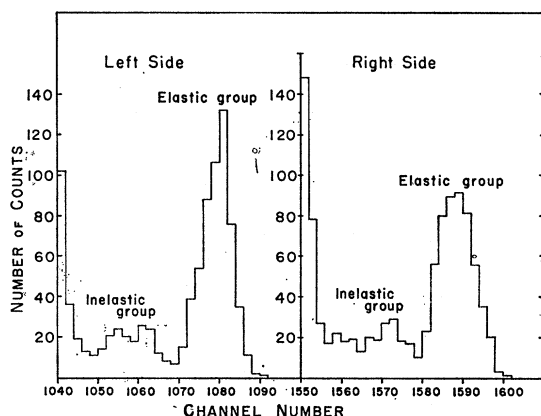


FIG. 1. Proton spectrum of the right and left scintillation counters at $\theta_{c.m.} = 41.1^\circ$.

B. Angular Distributions

The angular distributions of the elastically scattered deuterons and of the protons corresponding to the $\text{Ca}^{40}(d,p)\text{Ca}^{41}$ ground-state reaction were obtained using the same 18.5 mg/cm^2 target. The measured cross sections and polarizations correspond, therefore, to averages over the same energy range. The target thickness was determined before and after the experiment, both by weighing and by a direct measurement with a micrometer. All measurements agreed within the estimated error ($\pm 0.8 \text{ mg/cm}^2$). A 7.5 at.% oxygen contamination, found in the elastic scattering, was corrected for. The same contamination was observed in a check run several months later. The reason for the good stability of the target lay probably in the fact that it was relatively thick and was always kept under vacuum.

The elastically scattered deuterons were detected by means of a 1-mm thick solid-state detector. This thickness corresponds to the range of 12.5-MeV protons and 17-MeV deuterons. Thus no protons except the very few scattered in the detector could give rise to pulses as large as those from elastic deuterons. Contributions from α particles were also negligible, since the cross sections are small ($< 0.5 \text{ mb}$ at forward angles) and moreover, their energy spectrum is completely smeared out, owing to the thickness of the target and the high specific-energy loss of α particles. The acceptance angle of the detector was always smaller than $\pm 0.2^\circ$, the angular spread of the incident beam about $\pm 0.5^\circ$, and the root-mean-square angular spread due to multiple scattering in the target was estimated¹² to be, depending on target angle, 1.1° - 1.3° . At angles smaller than 30° the data were corrected for the limited angular resolution by means of the theory of Molière.¹² The correction at 10° amounted to 0.3° in angle or alternatively 10% in the cross section. The angular scale is believed to be accurate to about $\pm 0.2^\circ$ at $\theta_{lab} \leq 30^\circ$ and

to about $\pm 0.3^\circ$ for $\theta_{lab} > 30^\circ$. The acceptance angle of the Faraday cup was $\pm 4^\circ$, and it was estimated that, depending on target orientation, 2-3% of the deuterons were scattered out of the Faraday cup.

At angles larger than 42.5° the deuterons elastically scattered from a 7.5 at.% oxygen contamination could be well separated from the Ca peak; at smaller angles a correction was applied using measurements made by Low.¹³ The energy resolution was not sufficient to separate the deuterons originating from Ca isotopes other than Ca^{40} . Since these constitute only 3% of the target and since the angular distributions are roughly equal, it is expected that this does not influence the

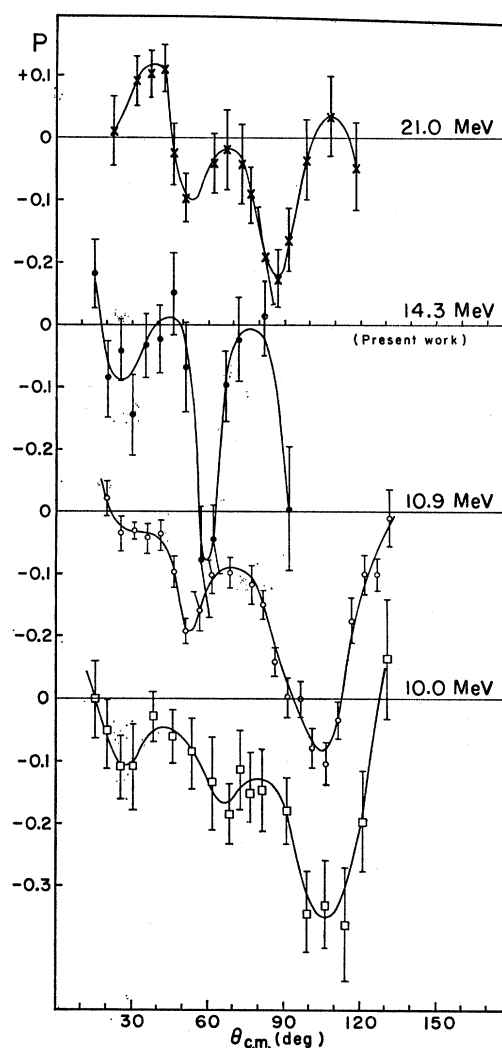


FIG. 2. Polarization of the protons in the reaction $\text{Ca}^{40}(d,p)\text{Ca}^{41}$ g.s. as obtained by various authors at different energies. The data at 10.0 MeV are from Ref. 4, at 10.9 from Ref. 5, at 14.3 present work, and at 21.0 MeV from Ref. 8. The curves shown are smooth curves drawn through the data points.

¹² R. D. Birkhoff, *Handbuch der Physik*, edited by S. Flügge (Springer-Verlag, Berlin, 1958), Vol. 34, p. 53.

¹³ C. A. Low, Jr., M. S. thesis, University of Pittsburgh, 1961 (unpublished).

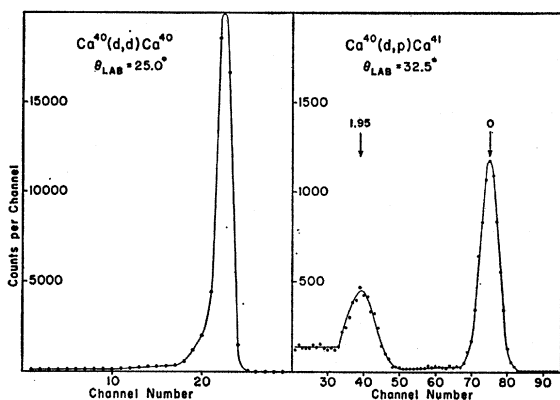


FIG. 3. Typical proton and deuteron spectra.

angular distribution appreciably except maybe in the diffraction minima.

For the (d,p) measurements, the protons were first energy degraded by means of a $\frac{1}{8}$ -in. thick polyethylene absorber and then detected with the same 1-mm solid-state detector. This arrangement had the advantage of eliminating the severe counting rate problem at forward angles, since the elastic deuterons were completely stopped in the absorber. An estimate was made of the loss of protons in the polyethylene absorber due to reactions and scattering from carbon and hydrogen. The elastic cross sections were obtained from Refs. 14 and 15 and the reaction cross section for C^{12} was taken from an optical-model analysis of elastic-scattering data.¹⁶ The absorption of protons was found to be approximately 1.5% and is thus of the same order of magnitude but of opposite sign as the error in the beam integration owing to scattering out of the Faraday cup.

The pulse-height spectra were recorded in a Nuclear Data 512-channel analyzer. Typical proton and deuteron spectra are displayed in Fig. 3. Dead time corrections were made possible by simultaneous recording of the pulses from a pulse generator and were always smaller than 7%.

Some time after the experiment was completed it was realized that there may have been spots in the detector, which were not fully depleted. There are indications of a low-energy tail in the pulse-height distribution of the elastically scattered deuterons, which could be interpreted in this way. Although the height of this tail is always 100 times smaller than the elastic peak, the total contribution could be as high as 10%. This uncertainty is the major source of error in the absolute cross sections. In light of this, no corrections were applied for integration and absorption losses.

The results of the angular-distribution measurements are displayed in Table II and Table III, and the

¹⁴ W. W. Daehnick and R. Sherr, Phys. Rev. **133**, B934 (1964).

¹⁵ N. Jaramie and J. D. Seagrave, Report No. LA-2014, 1957 (unpublished).

¹⁶ J. S. Nodvik, C. B. Duke, and M. A. Melkanoff, Phys. Rev. **125**, 975 (1962).

TABLE II. Differential cross sections in mb/sr for $Ca^{40}(d,d)Ca^{40}$ at 14.3 MeV.

$\theta_{e.m.}$	σ	σ/σ_R	$\theta_{e.m.}$	σ	σ/σ_R
10.6	28700	0.759	50.0	34.9	0.403
11.6	18150	0.688	52.6	29.10	0.407
13.3	11700	0.765	55.2	25.90	0.433
14.4	6950	0.624	57.8	23.60	0.466
15.9	4715	0.628	60.3	21.60	0.500
17.0	4130	0.716	62.9	19.15	0.515
18.6	3130	0.759	65.5	16.30	0.505
21.3	1687	0.715	68.0	13.28	0.470
22.3	1300	0.661	70.5	9.88	0.396
23.9	814	0.543	73.1	6.36	0.289
26.5	403	0.405	75.6	4.15	0.211
29.1	207	0.300	78.2	2.58	0.147
31.7	112	0.227	80.7	1.95	0.123
34.4	81.6	0.227	83.2	2.10	0.147
37.0	73.7	0.272	85.2	2.62	0.203
39.6	71.2	0.341	88.3	3.47	0.294
42.2	64.2	0.394	90.8	4.22	0.391
44.8	54.9	0.421	93.3	4.76	0.479
47.4	44.0	0.415			

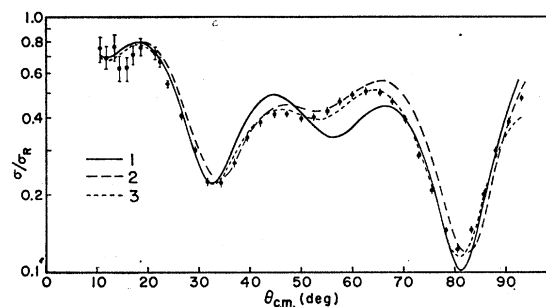
TABLE III. Differential cross sections in mb/sr for $Ca^{40}(d,p)Ca^{41}$ g.s. at 14.3 MeV.

$\theta_{e.m.}$	σ	$\theta_{e.m.}$	σ
11.0	1.45	47.0	2.15
13.7	2.10	52.1	1.50
16.2	2.80	57.2	1.44
21.3	4.31	62.3	1.55
26.5	5.65	67.3	1.52
29.0	6.06	72.4	1.39
31.6	6.13	77.4	1.21
34.2	5.78	82.5	1.08
36.8	5.12	87.5	0.89
41.9	3.37	92.5	0.74

TABLE IV. A summary of the estimated errors in the cross-section measurements. The large errors at $\theta_{e.m.} \approx 11^\circ$ goes continuously over in the typical large-angle errors at $\theta_{e.m.} = 25^\circ$ and 20° , respectively. All errors are in percent.

	$Ca(d,d)Ca$ $\theta_{e.m.} \approx 11^\circ$	$Ca(d,d)Ca$ $\theta_{e.m.} > 25^\circ$	$Ca^{40}(d,p)Ca^{41}$ $\theta_{e.m.} \approx 11^\circ$	$Ca^{40}(d,p)Ca^{41}$ $\theta_{e.m.} > 20^\circ$
Relative error rms	13	3	6	3
Absolute error rms	16	9	10	9

estimated errors are summarized in Table IV. Graphs of the results of the (d,d) measurement appear in Figs. 4 and 5 and of the (d,p) measurement in Figs. 7–11.

FIG. 4. Optical-model fits to the elastic scattering of 14.3-MeV deuterons by Ca^{40} using potentials Nos. 1, 2, and 3 of Table V.

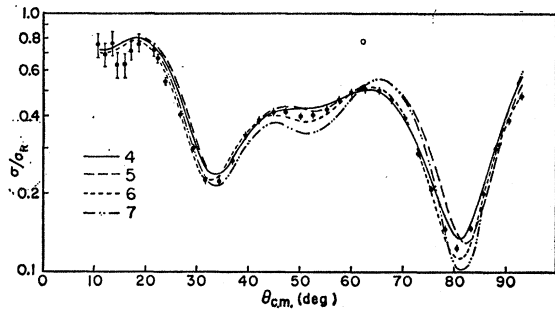


FIG. 5. Optical-model fits to the elastic scattering of 14.3-MeV deuterons by Ca^{40} using potentials No. 4, 5, 6, and 7 of Table V.

The error bars in Figs. 4 to 11 indicate the relative errors as summarized in Table IV.

III. THEORETICAL ANALYSIS

The theoretical analysis to be reported here is preliminary in the sense that the optical-model parameters required are far from being unambiguously determined at the present time. Part of the difficulty with the deuteron parameters is that an analysis of the differential cross section alone is insensitive to the form and strength of the spin-orbit coupling. Although extensive polarization measurements are available¹⁷ for 22-MeV deuterons on Ca^{40} , there still remains the problem of finding a potential to fit these data which is consistent (within the small energy variations expected) with the data reported here and other lower

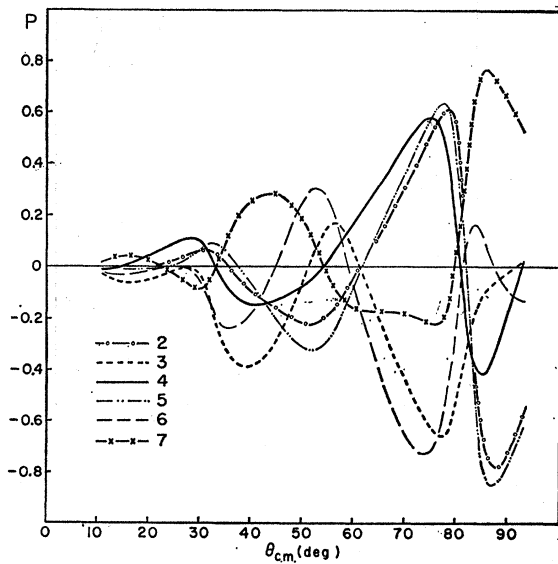


FIG. 6. Vector-polarization predictions for the elastic scattering of 14.3-MeV deuterons by Ca^{40} using the potentials of Table V.

energy data. This problem is only partially solved,¹⁸ and work on it is continuing.

The proton potential required is that for scattering from Ca^{41} , whereas data are available only for targets of Ar^{40} , Ca^{40} , and Ca^{42} , and other neighboring nuclei. Normally this would not be regarded as a serious problem, although there have been suggestions¹⁹ that the potential for Ca^{40} shows closed-shell effects and, if this is so, it is not clear to what extent they may still be present for Ca^{41} . Further, while there are preliminary

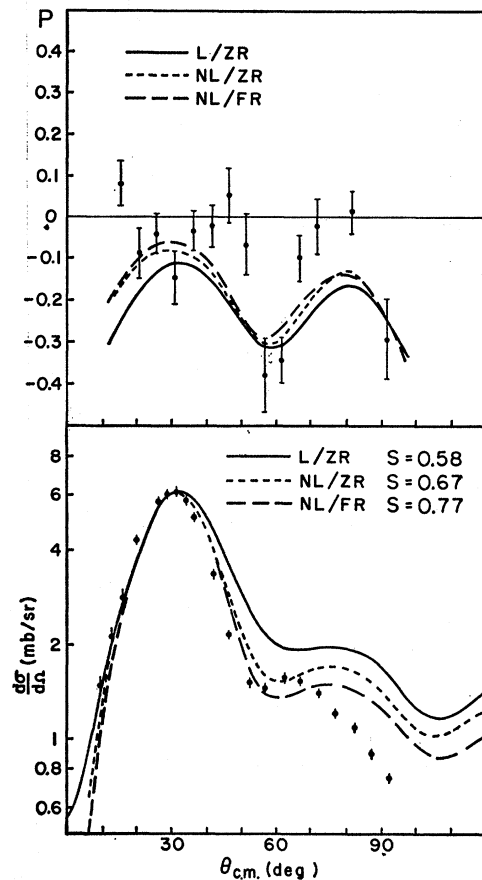


FIG. 7. Differential cross sections and polarizations for $\text{Ca}^{40}(d, p)$ at 14.3 MeV. The theoretical curves use deuteron potential No. 8 and proton potential No. 1 to illustrate the effects of finite range and nonlocality. L and NL mean local and nonlocal; ZR and FR mean zero and finite range, respectively.

results of elastic polarization measurements²⁰ for protons of 18 MeV on K^{39} and of 16.6, 18.2, and 21 MeV on Ca^{40} , the analysis of these is equally preliminary and has not yet yielded a potential in which we can have complete confidence. In particular, it is not yet clear whether the data demand the spin-orbit coupling to be complex, or require its radius and diffuseness to differ from those

¹⁷ R. Beurtey *et al.*, *Compt. Rend.* **256**, 922 (1963); **257**, 1267, 1477 (1963).

¹⁸ J. Raynal, *Phys. Letters* **7**, 281 (1963).

¹⁹ H. C. Volkin, *Bull. Am. Phys. Soc.* **9**, 439 (1964).

²⁰ E. Boschitz (private communication).

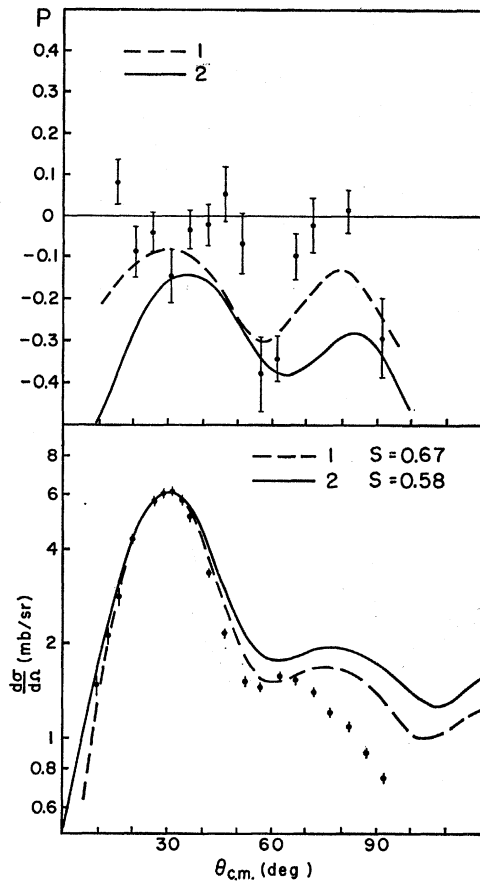


FIG. 8. Comparison of predictions for $\text{Ca}^{40}(d,p)$ using proton potentials No. 1 and 2. Deuteron potential No. 8 was employed, and the calculations made using the zero-range approximation. Nonlocal corrections were included.

of the central potential. For this reason, attention will be concentrated on results using the proton potential which was employed in the recent analysis³ of the $\text{Ca}^{40}(d,p)$ reaction at energies of 7 to 12 MeV. This potential gives a good account of the elastic scattering from Ca^{42} at 12 MeV and from Ar^{40} at 8 to 12 MeV, and, in addition, qualitatively reproduces the preliminary proton polarization data for K^{39} and Ca^{40} . Calculations have been performed using potentials adjusted to obtain fits to the latter data, but no dramatic improvements in the fits to the (d,p) data are found.

A. Elastic Deuteron Scattering

The optical potentials used in the present analyses have the form

$$U(r) = U_c(r) - V(e^x + 1)^{-1} + 4iW_D(d/dx')(e^x + 1)^{-1} + (\hbar/m_\pi c)^2(V_s + iW_s)(d/dr)(e^x + 1)^{-1} \mathbf{L} \cdot \boldsymbol{\sigma}, \quad (1)$$

where

$$x = (r - r_c A^{1/3})/a, \quad x' = (r - r'_c A^{1/3})/a',$$

and $U_c(r)$ is the Coulomb potential from a uniform

charge of radius $r_c A^{1/3}$. For protons, $\boldsymbol{\sigma}$ is the Pauli spin- $\frac{1}{2}$ operator, while for deuterons, $\boldsymbol{\sigma}$ is the spin-1 operator. An automatic search routine was used to vary the parameters of this potential so as to optimize the fit to experiment.²¹ Since rather little is known about the spin-orbit coupling for deuterons, fits were obtained without it, and with real, imaginary, and complex spin-orbit strengths, in order to study their various effects on the predictions for the deuteron stripping.

There are known to be other ambiguities in the choice of optical-model parameters for deuterons; in particular, a whole series of potentials can be found which differ, crudely, only in the number of half-wavelengths which are included in the well.^{2,21,22} However, the recent analysis³ of $\text{Ca}^{40}(d,p)$ measurements at energies of 7 to 12 MeV gave some reasons for preferring the potentials whose real part was approximately 100 MeV deep,

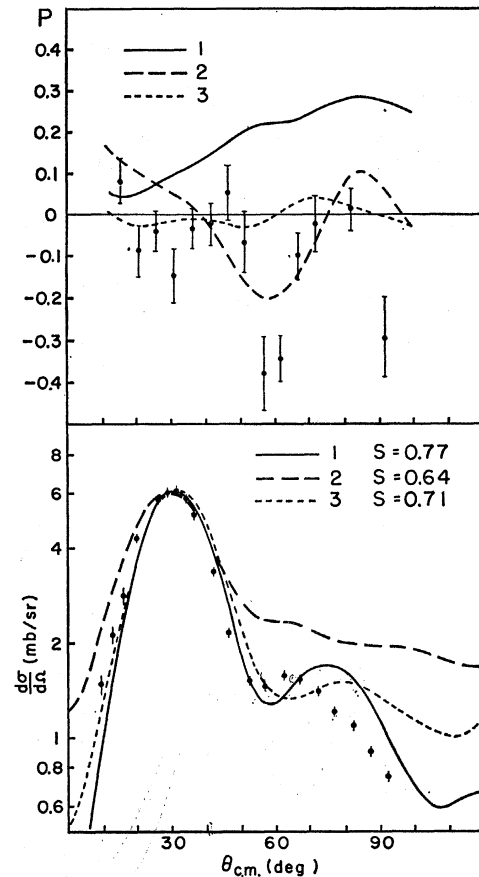


FIG. 9. $\text{Ca}^{40}(d,p)$ predictions with real and imaginary spin-orbit coupling for the deuterons, with and without, in the zero-range approximation but including nonlocal corrections. Proton potential No. 1 was used. The numbers refer to the deuteron potentials of Table V.

²¹ R. M. Drisko (unpublished). See also E. C. Halbert, Nucl. Phys. **50**, 353 (1964); C. M. Perey and F. G. Perey, Phys. Rev. **132**, 755 (1963).

²² R. M. Drisko, G. R. Satchler, and R. H. Bassel, Phys. Letters **5**, 347 (1963).

and for this reason efforts were concentrated on this class of potentials. In addition, one example each of a potential shallower and deeper than this was also obtained. Another ambiguity concerns the radial distribution of the absorptive potential. The form (1) assumes a surface-peaked shape, but it is known that equally good fits can be obtained with volume absorption.^{2,21} This ambiguity is known to have little effect on the predictions of the deuteron-stripping cross sections,³ and studies with the present data showed that it has little effect on the polarization predictions also.

The parameters for these various potentials are indicated in Table V, and comparisons between experiment and the corresponding optical-model fits are shown in Figs. 4 and 5. The corresponding predictions for the vector polarization are shown in Fig. 6. Other data for deuteron scattering from Ca^{40} at 14.9 MeV have become available recently²³ which are less complete at the forward angles but extend out to 166° (c.m.). Analysis of these data have yielded potentials similar

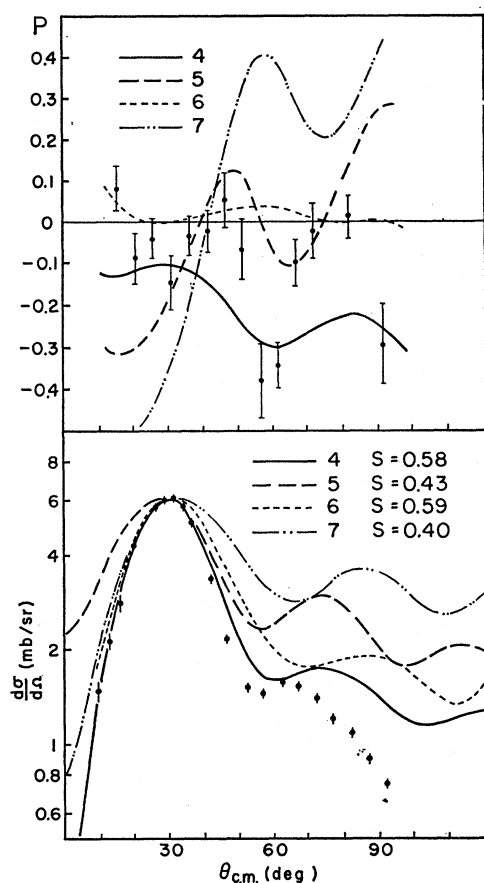


FIG. 10. $\text{Ca}^{40}(d, p)$ predictions with various combinations of real and imaginary parts for the deuteron spin-orbit strength; the numbers refer to the potentials of Table V. Proton potential No. 1 was used. The zero-range approximation was made, but nonlocal corrections were included.

²³ W. Daehnick (private communication).

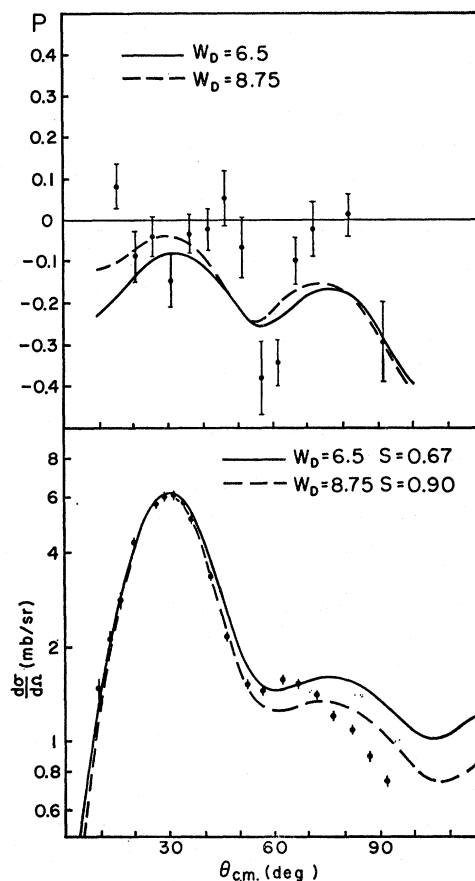


FIG. 11. $\text{Ca}^{40}(d, p)$ predictions using the deuteron potential No. 8 ($W_D=6.5$) and the same potential except with W_D increased to 8.75. Proton potential No. 1 was used and the zero-range approximation made, but nonlocal corrections were included.

to those found at 14.3 MeV, except for an increase of roughly 30% in the absorptive strength. The potentials obtained at 14.3 MeV predict much too large a cross

TABLE V. Optical-model parameters.^a

	V	r_0	a	W_D	r_0'	a'	V_S	W_S	
	(MeV)	(F)	(F)	(MeV)	(F)	(F)	(MeV)	(MeV)	χ^2 ^b
Proton									
No. 1	51.0	1.20	0.65	11.0	1.25	0.47	7.5	0	...
2	50.0	1.20	0.65	8.0	1.25	0.47	4.0	1.0	...
Deuteron									
No. 1	98.6	1.112	0.875	17.3	1.562	0.477	0	0	144
2	146.7	0.810	0.882	6.5	1.590	0.663	7.58	0	81
3	95.6	1.119	0.928	14.6	1.529	0.499	0	6.95	24
4	122.3	0.957	0.778	5.2	1.605	0.804	8.36	3.59	54
5	139.3	0.836	0.881	6.4	1.611	0.677	9.16	-1.43	77
6	124.1	0.896	0.993	8.6	1.540	0.718	-5.75	4.84	25
7	130.7	0.876	0.942	7.2	1.562	0.673	-8.79	-3.04	65
8 ^c	114.5	0.997	0.808	6.5	1.611	0.706	9.49	2.73	27
9 ^d	110.1	1.023	0.792	7.9	1.618	0.635	8.39	1.61	36
10 ^e	67.5	0.944	0.946	6.3	1.641	0.668	7.48	0	25
11 ^e	162.1	1.058	0.784	12.2	1.546	0.536	11.06	0	56

^a The charge radius $r_c=1.25$ F for protons, $r_c=1.30$ F for deuterons.

^b Assuming 20% errors at the first 9 angles, 10% at the 35 other angles.

^c Data increased by 10%.

^d Data increased by 20%.

section at the wide angles at 14.9 MeV, and this increase in absorption is required to bring the cross section down into agreement with the experiment. It is then found that the optimum potential at 14.9 MeV produces only qualitative agreement with the 14.3-MeV data at forward angles; in particular, the ratio of the two peaks at 45° and 65° is incorrectly predicted. It does appear, however, that the two sets of data can be fitted by a single potential if the cross sections for both are increased by between 10% and 20% in magnitude. This is within the expected errors of normalization for the two sets of measurements. Examples are included in Table VI of optimum fits to the 14.3-MeV data when it is increased by 10% and 20%. It will be noted that, at least for this choice of spin-orbit coupling, the deviation χ^2 between experiment and theory is also a minimum for a renormalization between these two values. Further work is under way to find a consistent optical-model description of these data and also those taken at 11.8 MeV²⁴ and 22 MeV,¹⁷ in order to obtain better understanding of the (d,p) polarization data reported here and those taken at other energies.

B. Proton Optical Model

The proton optical potential used also has the form (1). Most of the analysis used the parameters (set 1 of Table V) which were also employed in the recent (d,p) analysis at 7 to 12 MeV and which give a good account of the scattering of 12-MeV protons from Ar⁴⁰ and Ca⁴². This potential has a real spin-orbit coupling term and gives a qualitative fit to the polarization measurements²⁰ for protons on Ca⁴⁰ and K³⁹. Somewhat better agreement with the latter measurements is obtained by using a complex spin-orbit strength (set of 2 Table V). Other proton potentials were used in exploratory calculations of the (d,p) reaction, including one with complex spin-orbit coupling whose radius and diffuseness parameters differed from those of the central potential. Since these led to no marked improvement in the fit to the (d,p) data, and in view of the current uncertainties over the details of the potential required to fit the proton scattering, these will not be discussed further here.

C. Distorted-Wave Calculation

The distorted-wave method has been discussed in detail elsewhere,²⁵ especially in relation to the Ca⁴⁰ (d,p) reactions at energies of 7 to 12 MeV.³ Calculations were performed for the present data using the potentials just described, mostly using the zero-range approximation. The neutron was assumed to be captured into an $1f_{7/2}$ orbit bound by 8.37 MeV in a Saxon well of radius $1.20A^{1/3}$ F and diffuseness 0.65 F, and with a

spin-orbit coupling 25 times the Thomas term. Although the optical potentials used were local, the damping of the wave functions in the nuclear interior which would arise from using equivalent nonlocal potentials²⁶ was included in the local energy approximation.²⁷ This approximation gives a damping factor of the form

$$f(r) = C[1 - \frac{1}{2}U(r)(m\beta^2/\hbar^2)]^{-1/2} \quad (2)$$

for each of the 3 wave functions appearing in the stripping amplitude. Here $U(r)$ is the corresponding local potential and β is the range of the nonlocality. The constant C is unity for scattering wave functions, but is adjusted to preserve the normalization for the bound-state wave function. The value $\beta = 0.85$ F was used for the neutron and proton, and $\beta = 0.54$ F for the deuteron. Since each factor $f(r)$ is roughly 15% less than unity in the nuclear interior, nonlocality results in a considerable reduction in the contributions from this region. However, $C > 1$ for the neutron bound state ($C = 1.13$ in the present case) so that there is a compensating increase in the contributions from the exterior region. Figure 7 shows the effect of this nonlocality correction in one case using deuteron potential No. 8. The fit to the angular-distribution peak is improved, and the spectroscopic factor needed is increased to 0.67, although this is still significantly smaller than the value of unity expected and the value of approximately 0.9 found at lower energies.³ The effect on the polarization is rather small, although it does reduce somewhat the discrepancy between experiment and theory.

Also shown in Fig. 7 is the effect of relaxing the zero-range approximation.²⁸ Finite-range corrections can also be computed in the local energy approximation,^{27,29} but this was not done in the present analysis because the accuracy of this approximation had not been fully checked. Rather, exact calculations were made using a Gaussian range function with range 1.25 F. The result again is a damping of the interior contributions and further slight improvements for both cross section and polarization. The spectroscopic factor is now increased to 0.77.

Figure 8 shows a comparison of the effects of the two proton potentials. The changes in the differential cross section can be traced to the smaller values of W_D for potential No. 2. Although quantitatively there are large differences in the polarization predicted, it is clear that making the proton spin-orbit strength complex has not introduced any new qualitative features. (It should be stressed that these two potentials do *not* give the same proton elastic scattering at this energy.)

²⁶ F. G. Perey, in *Proceedings of the Conference on Direct Interactions and Nuclear Reaction Mechanisms, Padua, 1962* (Gordon and Breach Publishers, Inc., New York, 1963).

²⁷ F. G. Perey and D. Saxon, *Phys. Letters* **10**, 107 (1964), and to be published.

²⁸ N. Austern, R. M. Drisko, E. C. Halbert, and G. R. Satchler, *Phys. Rev.* **133**, B3 (1964).

²⁹ P. J. A. Buttle and L. B. J. Goldfarb, *Proc. Phys. Soc. (London)* **A83**, 701 (1964).

²⁴ T. Becker, U. Schmidt-Rohr, and E. Tielsch, *Phys. Letters* **5**, 331 (1963).

²⁵ G. R. Satchler, *Nucl. Phys.* **55**, 1 (1964).

This is not true of the deuteron spin-orbit coupling. First, Fig. 9 shows that neglect of spin-orbit coupling for the deuteron gives a (d,p) polarization in complete disagreement with experiment. (Using finite range has negligible effect on the polarization but does improve the fit to the differential cross section. Indeed, in all cases studied the effect of finite range is very similar to that shown in Fig. 7). An imaginary spin-orbit coupling gives better agreement with experiment except that it does not reproduce the large polarizations observed near 60° and 90° . (However, it should be noted that the differential cross section is not reproduced correctly in these regions either; this difficulty was encountered at lower energies³ and persists throughout the present analysis.) The use of a real spin-orbit term alone brings about the required dip in the polarization around 60° but the fit to the cross section is not so good in this case.

Figure 10 illustrates the effects of taking various combinations of real and imaginary parts of the deuteron spin-orbit strength. Potentials No. 5 and 7 are clearly unacceptable, which would indicate a need for a positive imaginary part. Potential No. 4 gives a fair fit to the cross section (which would be improved with the inclusion of finite-range effects), and reproduces the large polarization values near 60° and 90° . Potential No. 6, on the other hand, misses these but gives a better account of the other polarization measurements; the fit to the cross section is distinctly poorer. Further, there are indications that spin-orbit coupling with a negative real part is incompatible with the elastic polarization measurements at 22 MeV; certainly one would expect it to have the same, positive, sign as the spin-orbit coupling for nucleons.

It was suggested above that analysis of the 14.9-MeV elastic scattering required a larger absorptive strength, and that to obtain consistency with the 14.3-MeV results, both cross sections should be increased in magnitude by between 10 and 20%. To illustrate how this affects the stripping predictions, Fig. 11 shows curves using potential No. 8 (from the 14.3-MeV results increased by 10%), and the same potential except that W_D was increased from 6.5 to 8.75 MeV. (With slight readjustment of the other parameters, this latter potential gives a reasonable account of both sets of elastic data if both are increased by 20%.) The increased damping due to absorption provides a better fit to the angular-distribution peak and also yields a more reasonable value (0.90) for the spectroscopic factor. The polarization at forward angles is also in slightly better agreement with experiment.

IV. DISCUSSION

As was stressed at the beginning of the previous section, the theoretical analysis presented here is preliminary, largely because of uncertainties in our knowledge of the details of the optical potentials. An additional uncertainty concerns the possibility of tensor

forms of spin-orbit coupling for the deuteron³⁰ in addition to the vector type assumed here, although it was not found necessary to introduce these in order to explain¹⁸ the elastic polarization measurements at 22 MeV.

Within these uncertainties we may draw some tentative conclusions. First, from Fig. 9 *it is clear that the deuteron spin-orbit coupling has considerable effect on the (d,p) polarization*, and that the measurements require it. It is less easily to place conditions on the form of this coupling. If we emphasize the large, negative, polarization values around 60° and 90° , then we require real or real-plus-imaginary parts both of positive sign. However, we should also bear in mind that the present theory seems incapable of reproducing the detailed structure of the differential cross section in this angular region; the same difficulty is present at lower energies.³ If, then, more emphasis is placed on the polarization measurements close to the main peak of the differential cross section, we are led to regard potentials No. 3 and 6 more seriously. There are indications that a negative imaginary part of the deuteron spin-orbit coupling gives unacceptable results in any case.

Although the qualitative features of the (d,p) polarization curves seem to be determined by the form of deuteron spin-orbit coupling, as shown in Figs. 9 and 10, the details are sensitive to small changes in the other parameters. The finite-range and nonlocality effects are of the same order as those shown in Fig. 7 for all cases we have examined, and similarly Fig. 8 is characteristic of uncertainties associated with the proton potential.

The magnitudes predicted for the differential cross sections imply spectroscopic factors somewhat smaller than anticipated, and smaller than found at lower energies.³ It is possible this is due to an underestimate of the elastic cross sections and hence of the deuteron absorptive strength (see Fig. 11). The angular distributions are generally acceptable (when finite range and nonlocality are included) in the region of the main peak, except for potentials 5, 7, 10, 11.

ACKNOWLEDGMENTS

We are indebted to Dr. R. M. Drisko for helpful discussions and for making available the distorted-wave codes and the optical-model search code. We would also like to thank Dr. W. Daehnick for many helpful discussions, and Dr. F. G. Perey and Dr. J. K. Dickens for making available the nonlocality correction factors. The untiring help of P. F. Brown, B. E. Johansen, and P. R. Crowley in taking data is greatly appreciated as is the assistance of the cyclotron technical staff. The help of G. Fodor who prepared the target is also gratefully acknowledged.

³⁰ G. R. Satchler, Nucl. Phys. **21**, 116 (1960).